NO-flow tagging by photodissociation of NO_2. A new approach for measuring small-scale flow structures

Claus Orlemann, Christof Schulz *, Jürgen Wolfrum

Physikalisch-Chemisches Institut, Universität Heidelberg, INF 253, 69120 Heidelberg, Germany

Abstract

A new flow tagging technique was developed which visualizes small-scale flow structures by writing a spatial line of NO into an air flow homogeneously seeded with NO_2. The NO-line was generated by photodissociation of NO_2 at 308 nm using a XeCl excimer laser and was imaged by planar laser-induced fluorescence at various delays after its formation. With seeding levels of 600 ppm, signal-to-noise levels are shown to be sufficient for detecting the shifted structure at delays of up to 20 ms. The technique was used to resolve small scale turbulent flow structures within a quartz cell. © 1999 Elsevier Science B.V. All rights reserved.

1. Introduction

A number of different approaches for measuring flow patterns by molecular tracers have been published [1–10]. In contrast to particle or droplet seeding, molecular tracers show a better ability to follow flows with high velocity gradients. This circumvents typical problems with particle seeding where at high speeds and high turbulence tracking of the gas flow by particles may be poor. Homogeneously seeded flows allow investigation close to walls, where electrostatic forces may cause problems with window fouling, and in the center of turbulence elements, where it is difficult to inject particles due to centrifugal forces. Furthermore, molecular tracers allow uniform seeding even in large-scale facilities.

The contribution of the molecular tracer to the total mass flow is generally negligible, avoiding a significant alteration of the flow. On the other hand, diffusion plays an important role and causes dilution of tracers within the tagged volume element. Therefore molecular tracers are restricted to investigations at high flow velocities or small spatial scales but they are the best choice for applications which aim to study interactions between molecular and turbulent mixing.

Three different applications of molecular tracers are common: first, the Doppler shifts of LIF- or Raman-signals can be used to evaluate velocities. This has been shown in both seeded flows (e.g. by LIF of an NO seeded supersonic flow [7], LIF of iodine [3], LIF of sodium vapor [8]) and by Rayleigh [5] or Raman [2] scattering in unseeded flows. In inhomogeneously seeded flows, velocities or mixing are visualized by the detection of concentration gradients which are induced by partial or pulsed seeding of the gas flow, e.g. using acetone [9] or NO [10]. In

---

* Corresponding author. Fax: +49 6221 544255; e-mail: christof.schulz@urz.uni-heidelberg.de

pulsed configurations, however, altering the flow by the injection has to be carefully avoided. Due to the statistic nature of the structure of the tracer clouds, these techniques complicate measurements when well-defined starting conditions are required. In contrast, flow tagging techniques are based on the movement of structures which are generated within the flow by photo-induced processes. For unseeded flows, Miles et al. proposed RELIEF (Raman-excitation and laser-induced electronic fluorescence) of O_2 [4]. Boedeker measured velocities by H_2O photolysis and subsequent LIF detection of OH [1], and Ribarov et al. [6] showed an ozone tagging technique by imaging an ArF-Laser written line of O_3.

In the study presented here, air flows were homogeneously seeded with NO_2 at low concentrations (a few hundred ppm). By photodissociation of NO_2, NO was formed, which can be imaged by planar LIF at various delays after its generation. Whereas several other tracers disappear rather quickly due to energy transfer processes (from vibrationally excited molecules [4]) or high reactivity (in the case of OH [1]), due to small reaction cross-sections, NO is stable on the timescale of interest. Therefore, using NO, the displacements of volume elements can be imaged at longer times and larger distances compared to other techniques. Furthermore, with the molecular weight of NO being between that of N_2 and O_2 and diffusion coefficients close to nitrogen, NO turns out to be a good choice for characterizing the small-scale behavior of turbulent air flows.

2. Photophysics of NO_2

A well-defined spatial line of NO can easily be produced by photodissociation of NO_2. Jones and Bayes [11] state from measurements at 300 K and NO_2-pressures between 0.5 and 4 Torr that the overall dissociation quantum yield is constant and close to 2. An increase in either the N_2 or O_2 mol fraction was found to reduce the quantum yield due to altered kinetics [12,13]. Photodissociation occurs at wavelengths shorter than 398 nm, which corresponds to the NO_2 dissociation limit at 3.115 eV [14]. Nevertheless, absorption cross-sections of NO_2 vary over more than one order of magnitude for commercially available UV laser sources. At 308 nm, the absorp-

tion cross-section of NO_2 ($\sigma = 1.7 \times 10^{-19}$ cm^2/mol [15]) is about a factor of 2.5 below its maximum around 400 nm, which is compensated for by the high power output of a XeCl excimer laser. At 226 nm, the absorption cross-section is 3.9×10^{-19} cm^2/mol [15], leading to the production of additional NO by the detection laser beam. This contribution, however, is negligible since the pulse energy density of the detection beam is about three orders of magnitude weaker than that of the photodissociation beam.

In the photodissociation process, NO is either produced initially by

$$NO_2\left(X^2A_1\right) + h\nu \rightarrow NO(X^2\Pi) + O(^3P), \qquad (1)$$
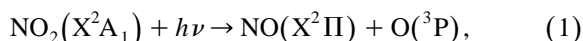
or at high NO_2 concentrations by the subsequent reaction of oxygen atoms

$$O(^3P) + NO_2\left(X^2A_1\right) \rightarrow NO(X^2\Pi) + O_2(X^3\Sigma). \qquad (2)$$
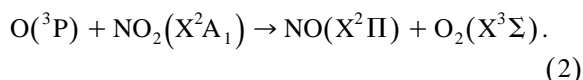
At atmospheric pressure and room temperature, the non-thermal vibrational populations after photodissociation [16–18] relax to the vibrational ground state within few nanoseconds. Therefore, in non-reactive flows, NO detection via LIF imaging requires excitation from the vibrational ground state.

The shape of the spatial line of NO is determined by the dissociation laser profile, but the NO-production channel (2) may cause a broadening of the line because of the diffusion of free oxygen atoms before attacking other NO_2-molecules. However, due to the low abundance of NO_2 in our experiments (a few hundred ppm) the contribution of channel (2) is expected to be negligible and the overall dissociation
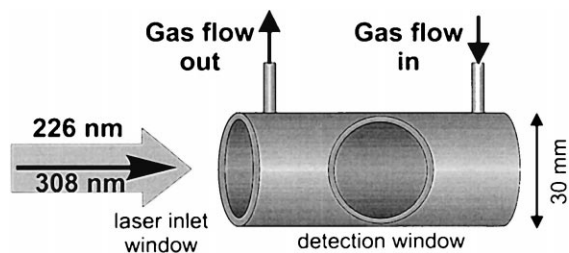
Fig. 1. Layout of the quartz cell in which both static and flow experiments were carried out. Main flow direction is from right to left, dissociation and detection laser were coupled in from the left side.

quantum yield is expected to be close to unity with NO formation occurring predominantly by reaction (1). With increasing pressure, in addition to mechanisms (1) and (2) the formation of NO_3 [12] via three-body reactions has to be considered. Then, the overall quantum yield of NO formation is further reduced [19,20] by

$$NO_3 + NO \rightarrow NO_2 + NO_2. \tag{3}$$
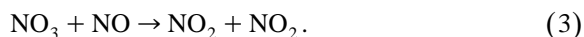
3. Experimental

Measurements were carried out in NO_2-seeded flows passing through a T-shaped quartz cell (Fig. 1). For photodissociation of NO_2, the beam of a XeCl excimer laser (308 nm, Lambda Physik EMG 150 TMC) was focused by a combination of two cylindrical lenses ($f = 2000$ mm and 500 mm, respectively). The resulting photodissociation beam had an average height of 0.8 mm and a width of 1 mm, resulting in energy densities of up to 225 MW/cm^2, which were varied with a dielectric attenuator. Imaging of room temperature NO usually was carried out with excitation of the A–X(0,0) transition at 226 nm [21]. The beam (1.3 mJ/pulse) of a XeF excimer-pumped (Lambda Physik LPX 200) frequency-doubled dye-laser (Lambda Physik, Scanmate IIe) was formed to a light sheet of 0.1 mm $\times$ 2.7 mm. LIF-signals of the NO A–X(0,1), (0,2) and (0,3) transitions (at 235–258 nm) were separated from scattered light by two dielectric mirrors acting as bandpass filters (Laseroptik, HR 248 nm at 45°, FWHM: 20 nm). Delays between the formation and detection of the NO-line were controlled by a pulse/delay generator (Stanford Research DG535). The spatial distri-

bution of NO was detected with a gated (100 ns) image-intensified slow scan CCD-camera (LaVision, Flame Star III) equipped with an achromatic lens (Halle, $f = 100$ mm, $f_\# = 2$). The arrangement of the optical system is shown in Fig. 2.

4. Generation of NO_2

Handling and controlling constant flows of NO_2 under atmospheric or higher pressure conditions is difficult due to condensation of NO_2 and formation of N_2O_x. Therefore, to provide constant and reproducible seeding, NO_2 was produced from the reaction of $NO + O_2$ by mixing NO (Messer Griesheim) with air in a 5 l steel chamber. The individual flows were controlled by mass flow controllers (Tylan FC 262) with a maximum flow of 100 slm and 66 sccm for air and NO, respectively. At standard conditions, the ratio of equilibrium concentrations of NO_2 and NO lies far on the side of NO_2. To give the system enough time to reach equilibrium, a second steel chamber of 50 l was used to increase residence times. The influence of the initial NO concentration and residence time on the signal-to-background ratio upon NO_2 photodissociation and NO-LIF detection was investigated.

5. Results and discussion

When detecting the NO generated by photodissociation of NO_2, the signal-to-background ratios are influenced in several ways. Therefore, the flow rates of NO and air had to be optimized regarding the points:

- The flow of the initial NO/air mixture should be slow enough to reach equilibrium inside the mixing chamber.
- The total number density of NO_2 and NO should be as low as possible to reduce fluorescence quenching and self absorption.
- Photodissociation of NO_2 should be very effective (close to saturation) in order to give high NO concentrations for increasing the signal-to-noise ratio of the LIF-detection.

In the gas mixing system, for practical reasons, the residence time of the mixture was limited to
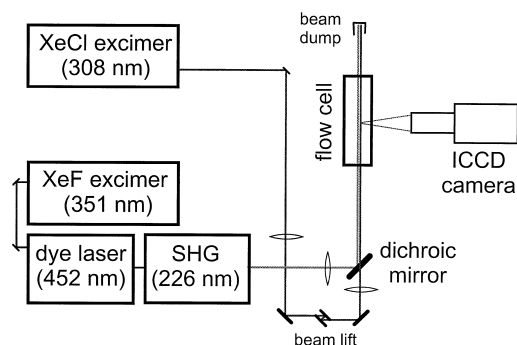
Fig. 2. Layout of the optical arrangement.

some minutes. The ratio of NO-LIF signals with and without photodissociation (at 308 nm) indicates the efficiency of the photodissociation process and determines the contrast between the dissociation induced NO-line and the detection laser sheet induced background. This was examined at different residence times of the seeding gases (NO/air mixture) inside the reaction vessel. At various flow rates which translate to average residence times from 1 up to 12 min, no significant increase in signal-to-background ratio was observed. This indicates that under the conditions used the NO/NO_2 equilibrium was reached within the residence times of the gas mixture in the reaction vessels.

NO fluorescence is efficiently quenched by NO_2. Doping the flow with high concentrations of NO_2 therefore does not necessarily increase signal intensities. Furthermore, increasing NO_2 and NO concentrations increases the attenuation of the laser beams and signal light. For our system, we found an initial flow of 27 slm air and 17 sccm NO gave optimal performance. Thus, the NO_2 concentration within the flow system under investigation could be as low as 600 ppm, which is also important with respect to the toxic and corrosive characteristics of NO_x. The energy density of the photodissociation laser beam should be high enough to dissociate every NO_2-molecule within the beam without inducing optical break-down and without damaging the windows. Fig. 3 shows the dependence of the LIF intensity from the generated NO-line versus the energy density of
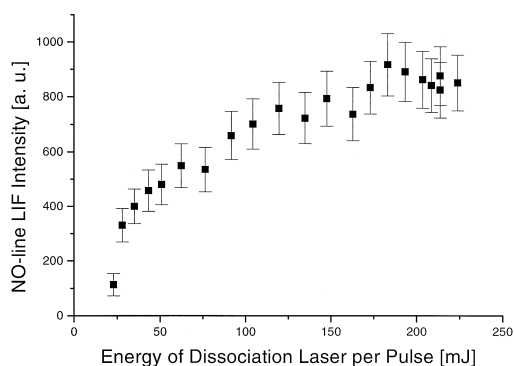
Fig. 4. Temporal evolution of the spatial width (FWHM) of the NO line.

the photodissociation beam (308 nm, XeCl excimer laser). As can be seen, the NO-signal rises linearly with energy densities up to approximately 100 MW/cm^2. Full saturation of the NO_2 photodissociation was observed above 180 MW/cm^2. For the experiment, a narrowband excimer laser was used. Due to its high beam quality, this laser allowed the beam to be focused tightly in order to cause photodissociation only within a small, well defined volume.

An important issue concerning the application range of a flow tagging technique is how far the effects of diffusion, which broaden the written line, are important. To test this, a $NO/NO_2/air$ mixture was filled into the quartz cell, allowing time to reach chemical equilibrium. Within the cell, the variation of the spatial width of the NO line was measured at different delays after photodissociation (Fig. 4). After 20 ms, the NO-line is broadened to 2 mm, but it still can clearly be discriminated against the background.

The new flow tagging technique was applied to the investigation of a turbulent flow inside a quartz cell. The narrow flow inlet tube (diameter: 4.5 mm) caused a fairly high Reynolds number of 8500 at flow rates of 27 slm. Vortex-street-like flow structures therefore allowed the testing of the abilities of the new flow tagging technique. Fig. 5 shows single-shot measurements at various temporal delays after writing a NO-line by photodissociation. The horizontal field of view is approximately 15 mm. In data evaluation, the image of the shifted line is divided by a reference image which shows energy

Fig. 3. Dependence of the NO-LIF intensity on the energy density of the dissociation laser beam. The intensities represent average values from a rectangular subregion around the center of the generated NO line. Error bars indicate the standard deviation of pixel intensities within this area.
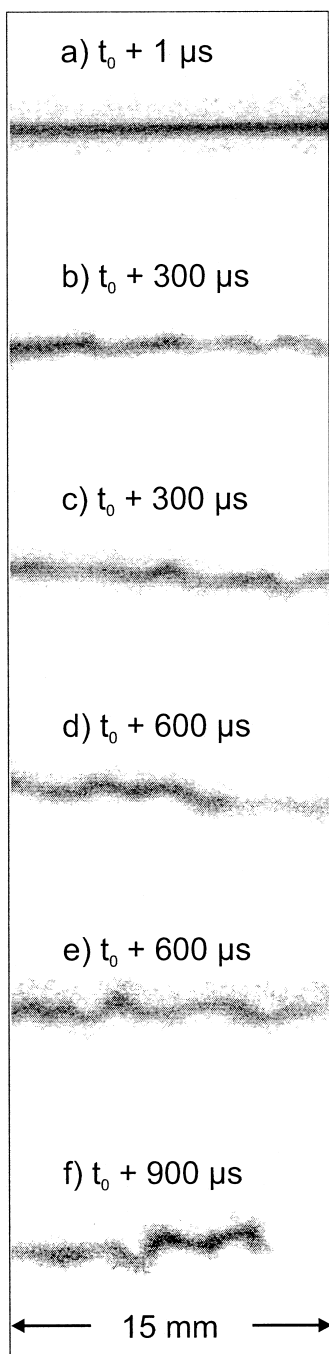
Fig. 5. Variation of the structure of the NO-line generated by photodissociation at various temporal delays.

line was segmented from the corrected image using a thresholding and erosion algorithm.

The resulting images show the statistical behavior of the highly turbulent flow. At a delay of 300 μs between dissociation and detection, the first oscillations of the line can be seen. These oscillations increase at longer delays, and pocket formation starts. The three-dimensional nature of the flow leads to interruption of the line when volume elements are moving out of the plane of detection.

6. Conclusions

The new NO/NO_2 flow tagging technique has been shown to be a promising tool for measuring small-scale flow patterns. NO_2 concentrations were optimized in order to maximize the signal-to-background ratios. Initial NO_2 concentrations of 600 ppm were found to give the best results. Constant NO_2 seeding was shown to be feasible, with NO_2 being formed within a 5 l mixing vessel and a 50 l delay vessel from the reaction of NO with air. Due to the long lifetime of the photochemically produced NO, marked volume elements can be traced at delay times as long as 20 ms. Dissociation laser energy densities of 180 MW/cm^2 per pulse generated with a XeCl excimer laser were shown to lead to optimal line-to-background contrast. A first application, monitoring a turbulent flow inside an odd geometry quartz cell shows highly resolved flow structures in the sub-millimeter-range. Further improvements in image processing routines (contour averaging) will allow the evaluation of low intensity structures. This will further extend the range of temporal delays accessible by the technique. In combination with highly focused dissociation laser beams, the spatial resolution can be extended down to some tens of microns. Highly resolved studies in turbulent flows close to walls are under way.

Acknowledgements

inhomogeneities within the lightsheet and the contribution of background luminosity. The center of the

References

[1] L.R. Boedeker, Opt. Lett. 14 (1989) 473.

[2] R.J. Exton, M.E. Hillard, Appl. Opt. 25 (1986) 14.

[3] B. Hiller, R.K. Hanson, Appl. Opt. 27 (1988) 33.

[4] R.B. Miles, C. Cohen, J. Connors, P. Howard, S. Huang, E. Markovitz, G. Russell, Opt. Lett. 12 (1987) 861.

[5] R.B. Miles, W.R. Lempert, Ann. Rev. Fluid. Mech. 29 (1997) 285.

[6] L.A. Ribarov, J.A. Wehrmeyer, F. Batliwala, R.W. Pitz, P.A. DeBarber, AIAA-Paper 98-0513, 1998.

[7] P.H. Paul, M.P. Lee, R.K. Hanson, Opt. Lett. 14 (1989) 417.

[8] R.B. Miles, E. Udd, M. Zimmermann, Appl. Phys. Lett. 32 (1978) 317.

[9] A. Lozano, S.H. Smith, M.G. Mungal, R.K. Hanson, AIAA J. 32 (1993) 217.

[10] G. Grünefeld, A. Gräber, A. Diekmann, S. Krüger, P. Andresen, Combust. Sci. and Tech. 135 (1998) 135.

[11] I.T.N. Jones, K.D. Bayes, J. Chem. Phys. 59 (1973) 4836.

[12] H.W. Ford, N. Endow, J. Chem. Phys. 27 (1957) 1156.

[13] H.W. Ford, S. Jaffe, J. Chem. Phys. 38 (1963) 2935.

[14] G. Herzberg, Molecular Spectra and Molecular Structure, III. Polyatomic Molecules, Krieger Publishing, Malabar, 1988.

[15] W.B. DeMore, S.P. Sander, C.J. Howard, A.R. Ravishankara, D.M. Golden, C.E. Kolb, R.F. Hampson, M.J. Kurylo, M.J. Molina, NASA JPL Publication 97-4, 1997.

[16] H. Zacharias, K. Meier, K.H. Welge, in: J. Hinze (Ed.), Energy Storage and Redistribution in Molecules, Plenum, New York, 1983, p. 107.

[17] A. Doughty, G. Hancock, E.L. Moore, Chem. Phys. Lett. 274 (1997) 58.

[18] I.W.M. Smith, R.P. Tucket, C.J. Whitham, Chem. Phys. Lett. 200 (1992) 615.

[19] H. Gaedtke, J. Troe, Ber. Bunsenges. Phys. Chem. 79 (1974) 184.

[20] J. Troe, Ber. Bunsenges. Phys. Chem. 73 (1967) 906.

[21] J.M. Seitzman, G. Kychakoff, R.K. Hanson, Opt. Lett. 10 (1985) 439.